POTENTIAL OF IKONOS AND QUICKBIRD IMAGERY FOR ACCURATE 3D POINT POSITIONING, ORTHOIMAGE AND DSM GENERATION

H. Eisenbeiss , E. Baltsavias, M. Pateraki, L. Zhang
Institute of Geodesy and Photogrammetry, ETH-Hoenggerberg, CH-8093, Zurich, Switzerland - (ehenri, manos, maria, zhangli)@geod.baug.ethz.ch

Thematic Session 20 – Applications of High Resolution Data

KEY WORDS: IKONOS, QUICKBIRD, high resolution, radiometric preprocessing, sensor models, point positioning, orthoimage, DSM, accuracy analysis

ABSTRACT:
This paper describes the processing of IKONOS and QUICKBIRD imagery of two different datasets in Switzerland for analyzing the geometric accuracy potential of these images for 3D point positioning, and orthoimage and DSM generation. The first dataset consists of panchromatic and multispectral IKONOS and QUICKBIRD images covering the region of Geneva. In the second area around Thun with a height range of ca. 1650 m, the dataset consisted of a triplet and a stereo pair with an overlap of 50 %. In both areas, laser DTM/DSM existed and in Geneva also aerial orthoimages. GCPs with an accuracy of 0.2-0.4 m have been used in both sites. The investigations for 3D point positioning included 4 different sensor models, different GCP measurement, variable number of control points and area covered by them. The results showed that the Rational Polynomial Coefficient (RPC) model compared to 2D and 3D affine models are more general and can model sufficiently imaging modes that depart from linearity. This is particular so for QUICKBIRD which needs after the use of RPCs an additional affine transformation in order to reach accuracies of 1m or less. With sufficient modeling, the planimetric accuracy was 0.4 – 0.5 m, even for few GCPs and only partly covering the images. Orthoimages were generated from both QUICKBIRD and IKONOS with an accuracy of 0.5-0.8 m, using a laser DTM. A sophisticated matching algorithm was employed in Thun. In spite of various difficult conditions like snow, long shadows, occlusions due to mountains etc., the achieved accuracy without any manual editing, was 1-5 m depending on the landcover type, while in open areas it was about 1 m. Under normal conditions, this accuracy could be pushed down to about 0.5 m. Thus, IKONOS, and to a lesser degree QUICKBIRD, could be an attractive alternative for DSM generation worldwide.

1. INTRODUCTION

1.1 *Aims*

The topic of this paper is the analysis of the potential of IKONOS and secondary QUICKBIRD (QB) for 3D point positioning, orthoimage and DSM generation. Two test sites, in Geneva and Thun, were used with accurate reference data and partly different aims. In both projects, there was a cooperation with the Swiss Federal Office of Topography (swisstopo) and Space Imaging (SI). In Geneva, the final aim was the investigation whether high-resolution satellite (HRS) imagery can be used for updating the Swiss national maps at foreign border areas, which has as prerequisite the generation of accurate orthoimages. Another aim was the analysis of accuracy of IKONOS and QB for 3D point positioning and orthoimage generation using Rational Polynomial Coefficients (RPCs) and other simpler sensor models. The HRS orthoimages will be compared to alternative information sources regarding feature interpretation and mapping by the swisstopo. In Thun, the main aim was accuracy investigations of IKONOS for point positioning and DSM generation using a block of images (2 strips with 5 images) over a terrain with large height range and very variable landcover. The whole processing was performed exclusively with software based on good quality algorithms and developed at our Institute, most of it part of an operational software package for processing of linear array digital imagery.

1.2 *Datasets*

In Geneva, we used two slightly overlapping IKONOS images (west and east, each about 10 km x 20 km) and one QB image covering the eastern and 60% of the western IKONOS images. In Thun, one stereo pair (eastern part) and a triplet (western part) of IKONOS images (each image 10 km x 20 km) were used, with each image group acquired on the same day (see Table 1). The two strips in Thun had a ca. 50% overlap, and the triplet images were covered in about 70% of the area by snow, while all images had long shadows. The nadir image in the triplet was very close to one image of the stereopair, which had a suboptimal base/height ratio. All IKONOS images were Geo, 11-bit with DRA off, with 1m panchromatic (PAN) and 4m multispectral (MS) channels (in Thun only PAN was used), while the QB image was Basic 1B, 11-bit, 0.63m PAN and 2.52m MS. IKONOS and QB images had associated RPC files. For the measurement of GCPs in the Geneva site we used in the Canton of Geneva orthoimages with 0.25 m pixel size and ca. 0.5 m accuracy, derived from 1 m laser DTM with 0.5 m accuracy and outside the Canton, Swissimage orthoimages with 0.5 m pixel size and 1 m accuracy, derived from a 25m DTM (DHM25) with ca. 2 m accuracy. The coordinates of the GCPs in Thun were measured with differential GPS. In all cases, GCPs were measured in the images semi-automatically using least squares and intersection of straight, long enough lines or ellipse fit. The control points have an accuracy of 0.2 - 0.4 m in object and image space. In Thun, a 2m laser DSM with an accuracy of 0.5 m - 1 m (1 sigma) for open areas and 1.5 m for vegetation areas was used as reference data for the DSM generation from IKONOS.

Image	Date of acquisition	Scanning mode	Sensor-Azimuth (deg)	Sensor-Elevation (deg)	Numbers of GCPs	GCP accuracy (m)	GCP measurement method
Geneva_Q	2003-07-29	Reverse	286.4	77.6	67	0.3-0.5	Orthoimage / laser DTM
Geneva_I_West	2001-05-28	Forward	253.6	67.2	34	0.3-0.5	Orthoimage / laser DTM
Geneva_I_East	2001-05-28	Reverse	240.2	61.6	44	0.3-0.5	Orthoimage / laser DTM
Thun_I_49_000	2003-12-11	Reverse	140.35	62.78	25	0.2-0.3	GPS

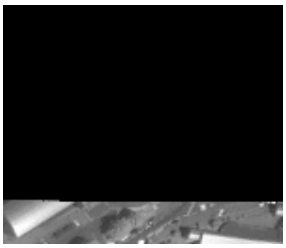

c) *d)*

Figure 1. Artefacts.

Spilling is probably the most grave radiometric problem, as it destroys image information and may confuse subsequent feature and object extraction. It increases with smaller pixel size and with smaller angle between the line-of-sight of the sensor and the reflected sun rays. It is pronounced because of the TDI and increases when more TDI stages are used. It is apparent that with bright targets the respective TDI pixels are saturated and the excess signal is not properly discharged, influencing subsequent lines. QB has much more spilling (more often, longer and wider) due to its smaller pixel size but also due to its continuous rotation during imaging. In Geneva, QB had 135 artifacts compared to 10 and 18 for IKONOS East and West. Ghosting of moving objects (Fig. 1 (d), QB) is visible in pansharpened images, due to the time difference in the acquisition of the PAN and MSI images. Another factor influencing image quality are shadows. In both IKONOS and QB images, most shadowed areas (especially in urban areas) did not have significant signal variation, even after strong contrast enhancement. However, in the winter images of Thun, very large open shadowed areas of mountain cliffs covered by snow could be enhanced quite successfully.

2.2 *Image Preprocessing*

In order to improve the radiometric quality and optimize the images for subsequent processing, a series of filters are applied. The performed preprocessing encompasses noise reduction, contrast and edge enhancement and reduction to 8-bit by non-linear methods. All filters are applied to the 11 bit data.

Noise reduction filters aim at reducing noise, while sharpening edges and preserving corners and one pixel wide lines. The two local filters employed have similar effects although they use different parameters (Baltsavias et al., 2001). In Fig. 2, the Adaptive Edge Preserving Weighted Smoothing is compared to a Gaussian filter. Apart from the visual verification, reduction of noise was quantified by noise estimation in inhomogeneous areas. Comparing Tables 3 and 4, a reduction of noise by a factor of about 2.5 - 3.0 and 1.8 for PAN IKONOS and QB, respectively, is estimated. Following noise reduction, local contrast enhancement is applied using the Wallis filter. Moreover, 11-bit data are reduced to 8-bit by an iterative non-linear method in order to preserve the grey values that are

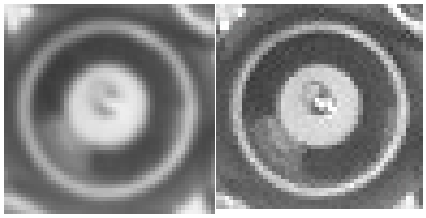

Figure 2. Effect of filtering: (left to right) Original image, Gaussian 5x5 filter, Adaptive Edge Preserving Weighted Smoothing.

PAN Scenes	**0 – 127**	**128 – 255**	**256 – 383**	**384 – 511**	**512 – 639**	**640 – 767**	**768 – 895**
Geneva_I	-	1.04	1.01	1.17	1.21	1.84	1.90
Geneva_Q	0.80	0.86	0.89	0.88	0.82	0.98	1.24
Thun stereo	0.53	0.54	1.56	2.55	-	-	-
Thun triplet	0.54	0.76	0.81	1.00	1.36	1.94	-

Table 4. Noise level in inhomogeneous areas and different grey value ranges (bins) for IKONOS scenes, after noise reduction.

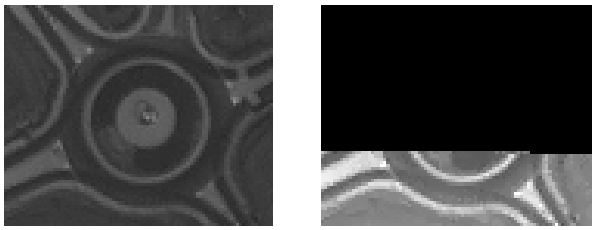

Figure 3. IKONOS image before (left) and after (right) preprocessing.

3. IMAGE ORIENTATION

3.1 *Methods and Sensor Models*

With the supplied RPCs and the mathematical model proposed by (Grodecki and Dial, 2003), a bundle adjustment is performed. The model used is:

$$x \quad x \quad x \quad a_0 \quad a_1 x \quad a_2 y \quad RPC\,(\ ,\ ,h)$$
$$y \quad y \quad x \quad b_0 \quad b_1 x \quad b_2 y \quad RPC_9(\ ,\ ,h)$$

where a_0, a_1, a_2 and b_0, b_1, b_2 are the affine parameters for each image, and (x, y) and (j, l, h) are image and object coordinates of points.

Using this adjustment model, we expect that a_0 and b_0 absorb most errors in the exterior and interior orientation. The parameters a_1, a_2, b_1, b_2 are used to absorb the effects of on-board GPS and IMU drift errors and other residual effects. In our approach, we first use the RPCs to transform from object to image space and then using these values and the known pixel coordinates we compute either two translations (model RPC1) or all 6 affine parameters (model RPC2).

For satellite sensors with a narrow field of view like IKONOS and QB, simpler sensor models can be used. We use the 3D affine model (3daff) and the relief-corrected 2D affine (2daff) transformation. They are discussed in detail in Fraser et al. (2002) and Fraser (2004). Their validity and performance is

expected to deteriorate with increasing area size and rotation of the satellite during imaging (which introduces nonlinearities), while the 3D affine model should perform worse with increasing height range and in such cases is more sensitive than the 2D affine model in the selection of GCPs.

3.2 *Measurements of the GCPs*

In Geneva, some roundabouts and more straight line intersections (nearly orthogonal with at least 10 pixels length) were measured semi-automatically in the satellite images and the aerial orthoimages (see Fig. 4). Measurement of GCPs by least squares template matching (Baltsavias et al., 2001) was not convenient or possible due to highly varying image content and scale. The height was interpolated from the DTM used in the orthoimage generation. An unexpected complication was the fact that the Canton of Geneva is using an own coordinate system and not the Swiss one! The transformation from one system to the other is not well defined, and based on different comparisons of transformed Geneva coordinates and respective coordinates in the Swiss system, a systematic bias has been observed, indicating that the results listed below could have been better. In Thun, the same image measurement approach was used, however, roundabouts (which are better targets) were very scarce. As expected, well-defined points were difficult to find in rural and mountainous areas, especially in Thun, where they had to be visible in 5 images simultaneously, while shadows and snow made their selection even more difficult. The object coordinates in Thun were measured with differential GPS. GPS requires work in the field, but the accuracy obtained is higher (espec. in height) and more homogeneous than using measurements in orthoimages, which have varying accuracy with unknown error distribution (due to the DSM/DTM). The number of GCPs and their accuracy are listed in Table 1.

Figure 4. Examples of GCP measurement with ellipse fitting (left) and line intersection (right).

3.3 *Comparison of different sensor models*

In Geneva, we compared various sensor models, IKONOS vs. QB and analysed the influence of the number of GCPs. Due to lack of space, only the most important results will be shown here.

Tables 5 and 6 show the results for the transformation from object to image space. Three different GCP configurations are used with all, 10 and 4 GCPs. Table 5 shows that with all GCPs, in IKONOS-East, all 4 sensor models have similar performance, with RPC2 being slightly better. In IKONOS-West (with forward scanning) results are similar for RPC1 and RPC2, a bit worse in y with 2D affine and considerably worse for 3D affine. The latter model deteriorates more with reduction of GCPs and is more sensitive to their selection. For the other models, the accuracy reduction from 44 to 4 GCPs is very modest, verifying findings from previous investigations that the number of GCPs is not so important, as their accuracy and secondary their distribution. The results for the 3D affine were initially by some factors worse than the ones of Table 5, when using geographic coordinates instead of map coordinates (oblique Mercator). The dependency of the results on the coordinate system has been discussed by Fraser (2004), albeit with smaller differences than the ones noted here.

Model	**GCP**	**CP**	**x-RMS [m]**	**y-RMS [m]**	**Max. D**x **[m]**	**max. D**y **[m]**
rpc1	44	-	0.65	0.56	1.40	1.21
rpc2	44	-	0.54	0.42	1.53	0.98
3daff	44	-	0.55	0.41	1.40	0.81
2daff	44	-	0.55	0.47	1.39	1.18
rpc2	10	34	0.57	0.52	1.52	1.07
rpc2	4	40	0.60	0.50	1.63	1.13
rpc1	4	30	0.63	0.40	1.35	1.40
rpc2	4	30	0.61	0.54	1.63	1.13
3daff	4	30	1.25	4.16	3.83	15.70
2daff	4	30	0.66	0.83	1.39	1.32

Table 5. Comparison of sensor models and number of GCPs with IKONOS-East (Geneva). At the bottom, one example for IKONOS-West. CP are the check points.

QB (see Table 6) is much less linear than IKONOS (expected partly due to its less stable orbit and pointing, and continuous rotation during imaging). Only RPC2 performs with submeter accuracy and only with this model can QB achieve similar accuracy as IKONOS. A residual plot with RPC1 shows a very strong x-shear. The 2D and 3D affine transformations are totally insufficient for modelling. As with IKONOS, a reduction of the GCPs has not any significant influence with RPC2. Thus, using simple RPCs (as in most commercial systems), or even applying 2 shifts in addition, will not lead to very accurate results with QB. It should be noted here that the QB image was Basic, i.e. not rectified. It is expected that a rectified image will show a more linear behaviour, and the respective RPCs will be more stable.

Model	**GCP**	**CP**	**x-RMS [m]**	**y-RMS [m]**	**max. D**x **[m]**	**max. D**y **[m]**
rpc1	67	-	2.64	0.43	5.57	0.92
rpc2	67	-	0.44	0.43	1.06	0.93
3daff	67	-	12.96	7.47	28.52	22.11
2daff	67	-	8.26	4.83	19.49	15.53
rpc2	10	57	0.46	0.44	1.12	0.97
rpc2	4	63	0.49	0.57	1.34	1.23

Table 6. Comparison of sensor models and number of GCPs with QB. CP are the check points.

For the Thun dataset, the triplet and stereo images were used separately in a bundle adjustment to determine object coordinates (processing of all images together was not possible due to a program limitation). Several semi-automatically measured (with least squares matching) tie points were included. The results for the triplet are shown in Table 7. The previous conclusions were verified, while the 3D affine model was worse compared to Geneva, probably because of the larger height range. A new indication compared to the Geneva data refers to the height accuracy. This is clearly better with RPC2,

and seems to get worse with decreasing number of GCPs, at least for this area with large height differences.

As a next step, we checked the role of the area covered by the GCPs, using always 5 GCPs (Table 8). RPC1 gave more or less similar results in planimetry, verifying previous investigations with the 2D affine model. The height however, is more sensitive to the position of the area covered by the GCPs, deteriorating in accuracy when GCPs were only in flat areas. Surprisingly, RPC2 gives clearly worse results than RPC1, especially when GCPs cover only 1/3 of the image area. This has been also verified with the Geneva images. A possible explanation is that after the RPCs are used, the scales and shears of the affine transformation model very small residual model errors. If in addition the GCP measurements are noisy (see e.g. the particularly high RMS at the mountainous south-west where GCP definition was poor), and the area covered is small, then these parameters may easily take wrong values. Grodecki and Dial (2003) mention the need to use only a linear factor in flight direction if the strip is long (about > 50 km). In future investigations, we will

Figure 5. Edge matching results in Alpine area.

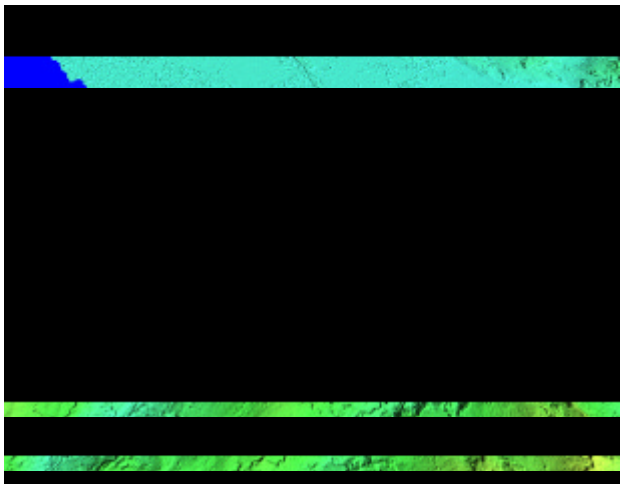

Figure 6. Shaded 5m DSM generated from IKONOS. The city of Thun in the upper left seen from North-West.

The procedure mainly contains the following characteristics:

1) It is a combination of feature point, edge and grid point matching. The grid point matching procedure uses relaxation-based relational matching, and can bridge-over areas with no or little texture through local smoothness constraints. The matched edges are introduced to control the smoothness constraints in order to preserve the surface discontinuities.
2) The adaptive determination of the matching parameters results in a higher success rate and less blunders. These parameters include the size of the matching window, the search distance and the threshold value for cross-correlation and MPGC. For instance, the procedure uses a smaller matching window, larger search distance and a smaller threshold value in rough terrain area and vice versa. The roughness of the terrain can be computed from the approximate DSM on a higher level of the image pyramid.
3) Linear features are important for preserving the surface discontinuities. A robust edge matching algorithm, using the multi-image information and adaptive matching window determination through the analysis of the image content and local smoothness constraints along the edges, is combined into our procedure. One example of edge matching is shown in Fig. 5.
4) Edges (in 3D) are introduced as breaklines when a TIN-based DSM is constructed. This DSM provides good approximations for matching in the next pyramid level. The computation of the approximate DSM in the highest pyramid level uses a matching algorithm based on the "region-growing" strategy (Otto and Chau, 1988), in which the already measured GCPs and tie points can be used as "seed points".
5) If more than two images are available, the MPGC procedure can use them simultaneously and matching results are more robust. Here, the resulting DSM from an image pair can be used as approximation for the MPGC procedure.
6) Through the quality control procedure, e.g. using the local smoothness and consistency analysis of the intermediate DSM at each image pyramid, the analysis of the differences between the intermediate DSMs, and the analysis of the MPGC results, blunders can be detected and deleted.

For each matched feature, a reliability indicator is assigned based on the analysis of the matching results from cross-correlation and MPGC. This indicator is used for assigning different weights for each measurement, which are used when a regular grid is interpolated.

4.2 *Test Results*

For Thun, we used for initial matching the images (and the respective triangulation results) of the triplet and stereopair separately and for the final MPGC all 5 images. The patch size varied from 7

Area	No. of Compared Points	Mean (m)	RMS (m)	< 2.0 m	2.0-5.0 m	> 5.0 m	Max. (m)
O+C+V+A	29,210,494	-1.21	4.80	60.7%	16.8%	21.3%	424.2
O+C+A	17,610,588	-1.11	2.91	77.0%	13.9%	10.1%	358.9
O+A	14,891,390	-1.24	2.77	79.8%	12.2%	8.0%	358.9
O	11,795,795	-1.00	1.28	90.3%	8.5%	1.2%	37.33

Table 9. Accuracy measures and error classes for the triplet. O-Open areas; C-City areas; V-Tree areas; A-Alpine areas.

Area	No. of Compared Points	Mean (m)	RMS (m)	< 2.0 m	2.0-5.0 m	> 5.0 m	Max. (m)
O+C+V	20,336,024	0.45	4.78	57.7%	21.3%	20.9%	125.2
O+C	13,496,226	-0.33	3.38	68.7%	20.8%	10.3%	47.34
O	3,969,734	-0.97	1.54	83%	15.0%	2.0%	39.4

Table 10. Accuracy measures and error classes for the stereopair. O-Open areas; C-City areas; V-Tree areas.

with cooperative texture. In fact in these areas, the matching accuracy was close to that of LIDAR.

5. CONCLUSIONS

The presented results verify that 3D points can be determined with a submeter accuracy which for the planimetry can be 0.5 m or less, if accurate GCPs are used. This was achieved also